

# A Stochastic Neural Network for Attack-Agnostic Adversarial Robustness

Panagiotis Eustratiadis<sup>1</sup>, Henry Gouk<sup>1</sup>, Da Li<sup>1, 2</sup>, Timothy Hospedales<sup>1, 2</sup>

<sup>1</sup>University of Edinburgh

<sup>2</sup>Samsung AI Center, Cambridge

{p.eustratiadis, t.hospedales, henry.gouk}@ed.ac.uk, da.li1@samsung.com

## Abstract

Stochastic Neural Networks (SNNs) that inject noise into their hidden layers have recently been shown to achieve strong robustness against adversarial attacks. However, existing SNNs are usually heuristically motivated, and further rely on adversarial training, which is computationally costly and biases models' defense towards a specific attack. We propose a new SNN that achieves state-of-the-art performance without relying on adversarial training, and enjoys solid theoretical justification. Specifically, while existing SNNs inject learned or hand-tuned isotropic noise, our SNN learns an anisotropic noise distribution to optimize a learning-theoretic bound on adversarial robustness. We evaluate our method on three benchmarks (CIFAR-10, SVHN, F-MNIST), show that it can be applied to different architectures (ResNet-18, LeNet++), and that it provides robustness to a variety of white-box and black-box attacks, while being simple and fast to train compared to existing alternatives. The source code is openly available on GitHub: <https://github.com/peustr/A2SNN>.

## 1 Introduction

It has been shown that deep convolutional neural networks, while displaying exceptional performance in computer vision problems such as image recognition (He et al. 2016), are vulnerable to input perturbations that are imperceptible to the human eye (Szegedy et al. 2014). The perturbed input images, known as adversarial examples, can be generated by single-step (Goodfellow, Shlens, and Szegedy 2015) and multi-step (Madry et al. 2018; Kurakin, Goodfellow, and Bengio 2017; Carlini and Wagner 2017) updates using both gradient-based optimization methods and derivative-free approaches (Chen et al. 2017). This vulnerability raises the question of how one can go about ensuring the security of machine learning systems, thus preventing a malicious entity from exploiting instabilities (Biggio, Fumera, and Roli 2013). In order to tackle this problem, many adversarial defense algorithms have been proposed in the literature (Liu et al. 2018, 2019; He, Rakin, and Fan 2019; Mustafa et al. 2019; Jeddi et al. 2020). Among them, Stochastic Neural Networks (SNNs) that inject fixed or learnable noise into their hidden layers have shown promising results (Liu et al. 2018; He, Rakin, and Fan 2019; Jeddi et al. 2020).

In this paper, we identify three limitations of the current state-of-the-art stochastic defense methods. First, most contemporary adversarial defense methods use a mixture of clean and adversarial samples during training, i.e. adversarial training (Goodfellow, Shlens, and Szegedy 2015; Madry et al. 2018; Liu et al. 2019; Mustafa et al. 2019; He, Rakin, and Fan 2019; Jeddi et al. 2020). However, generating strong adversarial examples during training leads to significantly higher computational cost and longer training time. More importantly, adversarial training assumes that the attack method is already known. However, it has been demonstrated that, though effective in improving robustness against a specific attack, maintaining robustness across different *unseen* attacks is a challenge (Shafahi et al. 2019). Second, many existing adversarial defenses (Mustafa et al. 2019), and especially stochastic defenses (Jeddi et al. 2020) are heuristically motivated. Although they may be empirically effective against existing attacks, they lack theoretical support. Third, the noise incorporated by existing stochastic models is *isotropic* (i.e. generated from a multivariate Gaussian distribution with a diagonal covariance matrix), meaning that it perturbs the learned features of different dimensions independently. Our theoretical analysis will show that this is a strong assumption and best performance is expected from *anisotropic* noise.

We address the aforementioned limitations and propose an attack-agnostic SNN (A<sup>2</sup>SNN) that makes use of learnable anisotropic noise. We theoretically analyse the margin between the clean and adversarial performance of a stochastic model and derive an upper bound on the difference between these two quantities. This novel theoretical insight suggests that the anisotropic noise covariance in an SNN should be optimized to align with the classifier weights, which has the effect of tightening the bound between clean and adversarial performance. This leads to an easy to implement regularizer, which can be efficiently optimized on clean samples alone without need for costly and attack-specific adversarial training. We show that our A<sup>2</sup>SNN can be applied to different architectures (namely, LeNet++ and ResNet-18), and achieves state-of-the-art performance across three widely used benchmarks, CIFAR-10, SVHN and F-MNIST. Moreover, this high level of robustness is demonstrated for both white-box and black-box attacks.

The contributions of our paper are summarized as follows:

- While the majority of existing stochastic defenses are heuristically motivated, our proposed method is derived by optimizing a learning theoretic bound, providing solid justification for its robust performance.
- To the best of our knowledge, we are the first to propose a stochastic defense with learned anisotropic noise.
- Our  $A^2SNN$  is attack-agnostic and only requires clean samples for training, unlike most of the current state-of-the-art defenses that require costly and attack-specific adversarial training.
- We demonstrate the state-of-the-art performance of our method on various benchmarks and show that  $A^2SNN$  is resilient to both white- and black-box attacks.

## 2 Related Work

### 2.1 Adversarial Attacks

We consider the standard threat model, where the attacker can construct norm-bounded perturbations to a clean input. First-order white-box adversaries use the gradient with respect to the input image to perturb it in the direction that increases misclassification probability. The attack can also be targeted or untargeted, depending on whether a specific misclassification is required (Goodfellow, Shlens, and Szegedy 2015; Kurakin, Goodfellow, and Bengio 2017; Madry et al. 2018; Carlini and Wagner 2017). By default, we consider the untargeted variants of these attacks. The simplest first-order adversary is the Fast Gradient Sign Method (FGSM), proposed in Goodfellow, Shlens, and Szegedy (2015). The attack adds a small perturbation to the input in the direction indicated by the sign of the gradient of the classification loss,  $\mathcal{L}$ , w.r.t. the input,  $\vec{x}$ , controlled by an attack strength  $\epsilon$ ,

$$\vec{x}' = \vec{x} + \epsilon \cdot \text{sign}(\nabla_{\vec{x}} \mathcal{L}(h(\vec{x}), y)),$$

where  $h$  is the target model. Kurakin, Goodfellow, and Bengio (2017) upgraded this single-step attack to a multi-step version named Basic Iterative Method (BIM) with iterative updates and smaller step size at each update. Though BIM works effectively, Madry et al. (2018) demonstrated that randomly initializing the perturbation generated by BIM, and then making multiple attempts to construct an adversarial example results in a stronger adversarial attack known as Projected Gradient Descent (PGD). Another white-box attack of slightly different nature is the C&W attack (Carlini and Wagner 2017), which aims to find an input perturbation  $\delta$  that maximizes the following objective:

$$\begin{aligned} & \mathcal{L}(h(\vec{x} + \delta), y) - \|\delta\|_p \\ \text{s.t. } & \vec{x} + \delta \in [0, 1]^n, \end{aligned}$$

where  $p$  is commonly chosen from  $\{0, 2, \infty\}$ .

Different from the white-box attacks, black-box attacks assume the details of the targeted model are unknown, and one can only access the model through queries. Therefore, in order to attack a target model in this case, one typically trains a substitute of it (Papernot et al. 2017) and generates an attack using the queried prediction of the target model and the

local substitute. Also, instead of training a substitute for the target model, zero-order optimization methods (Chen et al. 2017; Su, Vargas, and Sakurai 2019) have been proposed to estimate the gradients of the target model directly. In this paper, we show that our proposed method is attack-agnostic and demonstrates strong robustness against both white- and black-box attacks.

### 2.2 Stochastic Adversarial Defense

Recent work has shown that SNNs yield promising performance in adversarial robustness. This can be achieved by injecting either fixed (Liu et al. 2018) or learnable (He, Rakin, and Fan 2019; Jeddi et al. 2020) noise into the models. The idea behind Random Self Ensemble (RSE) (Liu et al. 2018) is that one can simulate an ensemble of virtually infinite models while only training one. This is achieved by injecting additive spherical Gaussian noise into various layers of a network and performing multiple forward passes at test time. Though simple, it effectively improves the model robustness in comparison to a conventional deterministic model.

RSE treats the variance of the injected noise as a hyperparameter that is heuristically tuned, rather than learned in conjunction with the other network parameters. In contrast, He, Rakin, and Fan (2019) propose Parametric Noise Injection (PNI), where a fixed spherical noise distribution is controlled by a learnable “intensity” parameter, further improving model robustness. The authors show that the noise can be incorporated into different locations of a neural network, i.e. it is applicable to both feature activations and model weights. The injected noise is trained together with the model parameters via adversarial training. Learn2Perturb (L2P) (Jeddi et al. 2020) is a recent extension of PNI. Instead of learning a single spherical noise parameter, L2P learns a set of parameters defining an isotropic noise perturbation-injection module. The parameters of the perturbation-injection module and the model are updated alternately in a manner named “alternating back-propagation” by the authors, using adversarial training.

Although conceptually related to the aforementioned stochastic defense methods,  $A^2SNN$  differs in several important aspects:  $A^2SNN$  is the first stochastic model to inject learnable *anisotropic* noise into the latent features. Our approach is derived from optimization of a learning theoretic bound on the adversarial generalisation performance of SNNs, which motivates the use of anisotropic noise.  $A^2SNN$  does not require adversarial training and can be optimized with clean samples alone, and is therefore efficient to train and attack-agnostic.

Another class of stochastic defenses apply noise to the input images, rather than injecting noise to intermediate activations (Pinot et al. 2019; Cohen, Rosenfeld, and Kolter 2019; Li et al. 2019; Lee et al. 2019). From a theoretical point of view, this can be seen as “smoothing” the function implemented by the neural network in order to reduce the amount the output of the network can change when the input is changed only slightly. This type of defense can be considered a black-box defense, in the sense that it does not actually involve regularizing the weights of the network—it only modifies the input. While interesting, it has primarily

been applied in scenarios where one is using a model-as-a-service framework, and cannot be sure if the model was trained with some sort of adversarial defense or not (Cohen, Rosenfeld, and Kolter 2019).

### 3 Method

Our proposed method, A<sup>2</sup>SNN, makes use of several techniques not found in prior work on SNNs for adversarial robustness. First, inspired by the noise regularization function proposed in Jeddi et al. (2020) we employ an entropy maximizing regularization term to increase the variety of noise injected into the network. Based on theoretical analysis of how the injected noise can impact generalisation performance, we propose a weight-covariance alignment loss term that encourages the weight vectors associated with the final linear classifier layer to be aligned with covariance matrix of the injected noise. Finally, further insight from the theory leads us to use anisotropic noise, rather than the isotropic noise typically employed by previous approaches.

Our method fits into the family of SNNs that apply additive noise to the penultimate activations of the network. Consider the function,  $f(\vec{x})$ , which implements the feature extractor portion of the network i.e. everything except the final classifier layer. Our A<sup>2</sup>SNN architecture is defined as

$$h(\vec{x}) = W(f(\vec{x}) + \vec{z}) + \vec{b}, \quad \vec{z} \sim \mathcal{N}(0, \Sigma),$$

where  $W$  and  $\vec{b}$  are the parameters of the final linear layer,  $\vec{z}$  is the vector of additive noise. The objective function used to train this model is

$$\mathcal{L} = \mathcal{L}_C - \lambda_1 \mathcal{L}_{ME} - \lambda_2 \mathcal{L}_{WCA}, \quad (1)$$

with  $\mathcal{L}_C$ ,  $\mathcal{L}_{ME}$ , and  $\mathcal{L}_{WCA}$  representing the classification loss (e.g. softmax composed with cross entropy), maximum entropy, and weight-covariance alignment loss terms, respectively.  $\lambda_1$  and  $\lambda_2$  are weights we select via grid-search. We describe each of our technical contributions in the remainder of this Section.

#### 3.1 Max-Entropy Regularization

Training a noise distribution to improve adversarial robustness runs into the risk of the noise degrading to a Dirac distribution, i.e. the variance is nullified. In order to prevent that, Jeddi et al. (2020) introduce a regularization technique to boost the learned variance during training (Eq. 8 in their paper). They empirically demonstrate that this regularization improves the robust performance of L2P.

Maximizing the variance of isotropic noise is equivalent to maximizing its entropy. In this paper, we introduce a maximum entropy loss with the same idea in mind, and use it as a regularization technique in our proposed method,

$$\mathcal{L}_{ME} = \frac{1}{2} \ln \det(2\pi e \Sigma). \quad (2)$$

#### 3.2 Weight-Covariance Alignment

Non-stochastic methods for defending against adversarial examples typically try to guarantee that the prediction for an input image cannot be changed. In contrast, a defense that

is stochastic should aim to minimize the probability that the prediction can be changed. In this Section, we present a theoretical analysis of the probability that the prediction of an SNN will be changed by an adversarial attack. For simplicity, we restrict our analysis to the case of binary classification.

Denoting a feature extractor as  $f$ , we define an SNN  $h$ , trained for binary classification as

$$h(\vec{x}) = \vec{w}^T(f(\vec{x}) + \vec{z}) + b, \quad \vec{z} \sim \mathcal{N}(0, \Sigma),$$

where  $\vec{w}$  is the weight vector of the classification layer and  $b$  is the bias. We denote the non-stochastic version of  $h$ , where the value of  $\vec{z}$  is always a vector of zeros, as  $\tilde{h}$ . The margin of a prediction is given by

$$m_h(\vec{x}, y) = yh(\vec{x}),$$

for  $y \in \{-1, 1\}$ . It is positive if the prediction is correct and negative otherwise.

The quantity in which we are interested is the difference in probabilities of misclassification when the model is and is not under adversarial attack  $\delta$ , which is given by

$$G_{p,\epsilon}^h(\vec{x}, y) = \max_{\vec{\delta}: \|\vec{\delta}\|_p \leq \epsilon} P(m_h(\vec{x} + \vec{\delta}, y) \leq 0) - P(m_h(\vec{x}, y) \leq 0). \quad (3)$$

Our main theoretical result, given below, shows how one can take an adversarial robustness bound,  $\Delta_p^h(\vec{x}, \epsilon)$ , for the deterministic version of a network, and transform it to a bound on  $G$  for the stochastic version of the network.

**Theorem 1.** *The quantity  $G_{p,\epsilon}^h(\vec{x}, y)$ , as defined above, is bounded as*

$$G_{p,\epsilon}^h(\vec{x}, y) \leq \frac{\Delta_p^h(\vec{x}, \epsilon)}{\sqrt{2\pi \vec{w}^T \Sigma \vec{w}}},$$

where the robustness of the deterministic version of  $h$  is known to be bounded as  $|\tilde{h}(\vec{x}) - \tilde{h}(\vec{x} + \vec{\delta})| \leq \Delta_p^h(\vec{x}, \epsilon)$  for any  $\|\vec{\delta}\|_p \leq \epsilon$ .

The proof is given in the supplemental material. We can see from Theorem 1 that increasing the bi-linear form,  $\vec{w}^T \Sigma \vec{w}$ , of the noise distribution covariance and the classifier reduces the gap between clean and robust performance. As such, we define the loss term,

$$\mathcal{L}_{WCA} = \sum_{i=1}^C \ln(\vec{w}_i^T \Sigma \vec{w}_i), \quad (4)$$

where  $C$  is the number of classes in the classification problem, and  $\vec{w}_i$  is the weight vector of the final layer that is associated with class  $i$ . We found that including the logarithm results in balanced growth rates between the  $\mathcal{L}_C$  and  $\mathcal{L}_{WCA}$  terms in Eq. 1 as training progresses, hence improving the reliability of training loss convergence.

The key insight of Theorem 1, operationalized by Eq. 4 is that the noise and weights should co-adapt to align the noise and weight directions. We call this loss Weight-Covariance Alignment (WCA) because it is maximized when each  $\vec{w}_i$  is well-aligned with the eigenvectors of the covariance matrix.

This regularization term runs into the risk of “accidentally” maximizing the magnitude of  $\vec{w}$ , rather than encouraging alignment or increasing the scale of the noise. To avoid this, after every update we enforce that each  $\vec{w}_i$  has unit norm by applying a projection function,

$$\vec{w}_i = \frac{1}{\|\vec{w}'_i\|_2} \vec{w}'_i,$$

where  $\vec{w}'_i$  is the non-projected weight vector for class  $i$  obtained directly after performing an update with SGD.

### 3.3 Injecting Anisotropic Noise

In contrast to previous work that only considers injecting isotropic Gaussian noise (Liu et al. 2019; He, Rakin, and Fan 2019; Jeddi et al. 2020), we make use of anisotropic noise, providing a richer noise distribution than previous approaches. Crucially, it also means that the principal directions in which the noise is generated no longer have to be axis-aligned. I.e., prior work suffers from the inability to simultaneously optimise alignment between noise and weights (required to minimise the adversarial gap bounded by Theorem 1), and freedom to place weight vectors off the axis (required for good clean performance). Our use of anisotropic noise in combination with WCA encourages alignment of the weight vectors with the covariance matrix eigenvectors, while allowing non-axis aligned weights, thus providing more freedom about where to place the classification decision boundaries.

Previous approaches are able to train the variance of each dimension of the isotropic noise via the use of the “reparameterization trick” (Kingma and Welling 2014), where one samples noise from a distribution with zero mean and unit variance, then rescales the samples to get the desired variance. Because the rescaling process is differentiable, this allows one to learn variance jointly with the other network parameters with backpropagation. In order to sample anisotropic noise, one can instead sample a vector of zero mean unit variance and multiply this vector by a lower triangular matrix,  $L$ . This lower triangular matrix is related to the covariance matrix as

$$\Sigma = L \cdot L^T.$$

This guarantees that the covariance matrix remains positive semi-definite after each gradient update.

## 4 Experiments

### 4.1 Experimental Setup

**Datasets** We demonstrate the performance of our A<sup>2</sup>SNN on three benchmarks: CIFAR-10 (Krizhevsky, Hinton et al. 2009), SVHN (Netzer et al. 2011) and Fashion-MNIST (Xiao, Rasul, and Vollgraf 2017). CIFAR-10 contains 60K 32x32 color images, 50K for training and 10K for testing. SVHN can be considered a more challenging version of MNIST (LeCun, Cortes, and Burges 2010); it contains almost 100K 32x32 color images of digits collected from Google’s Street View imagery, with roughly 73K for training and 26K for testing. Fashion-MNIST is a collection of 70K 28x28 grayscale images of clothing, 60K for training

and 10K for testing. In all three benchmarks the data points are evenly spread across 10 classes.

**Models** For CIFAR-10 and SVHN we use ResNet-18 (He et al. 2016) as the backbone, while for F-MNIST, being a relatively simple dataset, we use LeNet++ (Wen et al. 2016). For both backbones we add a 32-dimensional penultimate layer for dimensionality reduction. This enables us to always train a 32x32 covariance matrix regardless of the original dimensionality of the feature extractor<sup>1</sup>. The exact values for  $\lambda_1$  and/or  $\lambda_2$  (Eq. 1) are provided in the supplementary material.

**Attacks** We evaluate our method using three white-box adversaries: FGSM (Goodfellow, Shlens, and Szegedy 2015), PGD (Madry et al. 2018) and C&W (Carlini and Wagner 2017), and one black-box attack: the One-Pixel attack (Su, Vargas, and Sakurai 2019).

We parameterize the attacks following the literature (He, Rakin, and Fan 2019; Jeddi et al. 2020). More specifically, FGSM and PGD are set with an attack strength of  $\epsilon = 8/255$  for CIFAR-10 and SVHN, and  $\epsilon = 0.3$  for F-MNIST. PGD has a step size of  $\alpha = \epsilon/10$  and number of steps  $k = 10$  for all benchmarks as per He, Rakin, and Fan (2019). C&W has a learning rate of  $\alpha = 5 \cdot 10^{-4}$ , number of iterations  $k = 1000$ , initial constant  $c = 10^{-3}$  and maximum binary steps  $b_{\max} = 9$  same as Jeddi et al. (2020).

For the parameters of the One-Pixel attack we tried to replicate the experimental setup described in the supplementary material of Jeddi et al. (2020) for attack strengths of 1, 2 and 3 pixels. We followed their setup with population size  $N = 400$  and maximum number of iterations  $k_{\max} = 75$ . However, we noticed that the more pixels we added to our attack the weaker the attack became, which is counter-intuitive. We attribute that to the small number of iterations; every added pixel substantially increases the search space of the differential evolution algorithm, and 75 iterations are no longer enough to converge when the number of pixels is 2 and 3. Therefore we maintain a population size of  $N = 400$ , but increase the number of iterations to  $k_{\max} = 1000$ . We further clarify that for the differential evolution algorithm we use a crossover probability of  $r = 0.7$ , a mutation constant of  $m = 0.5$ , and the following criterion for convergence:

$$\sqrt{\text{Var}(\mathcal{E}(X))} \leq \left| \frac{1}{100N} \sum_{x \in X} \mathcal{E}(x) \right|,$$

where  $X$  denotes the population,  $\mathcal{E}(X)$  the energy of the population and  $\mathcal{E}(x)$  the energy of a single sample.

**Expectation over Transformation** Due to the noise injected by SNNs, the gradients used by white-box attacks are stochastic (Athalye, Carlini, and Wagner 2018). As a result, the true gradients cannot be correctly estimated for attacks that use only one sample to compute the perturbation. To avoid this issue, we apply Expectation over Transformation (EoT) following Athalye, Carlini, and Wagner (2018). When

<sup>1</sup>A 512x512 covariance matrix obtains identical performance.

Table 1: Comparison of state-of-the-art SNNs for FGSM and PGD attacks on CIFAR-10 with a ResNet-18 backbone. Performance of competing methods extracted from Jeddi et al. (2020).

Method	Clean	FGSM	PGD
Adv-BNN	82.15	60.04	53.62
PNI	87.21	58.06	49.42
L2P	85.30	62.43	56.06
A <sup>2</sup> SNN	84.40	73.29	72.05

Table 2: Comparison of state-of-the-art methods for C&W attack on CIFAR-10 with a ResNet-18 backbone. Performance of competing methods extracted from Jeddi et al. (2020).

Confidence	Adv-BNN	PNI	L2P	A <sup>2</sup> SNN
$\kappa = 0$	78.9	66.9	83.6	84.4
$\kappa = 0.1$	78.1	66.1	84.0	83.8
$\kappa = 1$	65.1	34.0	76.4	77.1
$\kappa = 2$	49.1	16.0	66.5	71.6
$\kappa = 5$	16.0	0.08	34.8	45.9

generating an attack, we compute gradients of multiple forward passes using Monte-Carlo sampling and perturb the inputs using the averaged gradient at each update. We empirically found that a reliable number of MC samples is 50 (as we observed performance begins to saturate from around 35 and converges at 40); thus, we use 50 across all experiments.

## 4.2 Comparison to Prior Stochastic Defenses

**Competitors** We compare the performance of A<sup>2</sup>SNN to three recent state-of-the-art stochastic defenses to verify its efficacy. **AdvBNN** (Liu et al. 2019): adversarially trains a Bayesian neural network for defense. **PNI** (He, Rakin, and Fan 2019): learns an “intensity” parameter to control the variance of their SNN. **Learn2Perturb (L2P)** (Jeddi et al. 2020): improves PNI by learning an isotropic perturbation injection module. All experiments use a ResNet-18 backbone and are conducted on CIFAR-10 for fair comparison.

**White-box Attack** We first compare our proposed A<sup>2</sup>SNN to the existing state-of-the-art methods in the white-box attack setting. From the results in Table 1, we can see that our A<sup>2</sup>SNN shows noticeable improvement,  $\sim 11\%$  and  $\sim 16\%$  on FGSM and PGD respectively, over the strongest competitor, L2P. Moreover, we find that our method does not sacrifice its performance on the clean data to afford such strong robustness. It is worth reiterating that our A<sup>2</sup>SNN is trained using clean samples alone and is not biased against any of these attacks at training. These results demonstrate the effectiveness and generality of our proposed method.

We also present the evaluation of our method against the C&W attack in Table 2. Here, the confidence level  $\kappa$  indicates the attack strength. From the results we can see that the performance of all the competitors degrades when the

Table 3: Comparison of state-of-the-art methods for One-Pixel Attack on CIFAR-10 with a ResNet-18 backbone. Performance of competing methods extracted from the supplementary material of Jeddi et al. (2020).

Attack Strength	Adv-BNN	PNI	L2P	A <sup>2</sup> SNN
Clean	82.15	87.21	85.30	84.40
1 pixel	68.60	50.90	64.45	75.55
2 pixels	64.55	39.00	60.05	73.28
3 pixels	59.70	35.40	53.90	69.14

Table 4: Comparison of A<sup>2</sup>SNN to recent state-of-the-art, both stochastic and non-stochastic, on CIFAR-10. All competitors evaluate their models on the untargeted PGD attack, with attack strength  $\epsilon = 8/255$ , and number of iterations  $k \in \{7, 10, 20\}$ . Some results are extracted from He, Rakin, and Fan (2019). AT: Use of adversarial training.

Defense	Architecture	AT	Clean	PGD
RSE (Liu et al. 2018)	ResNext	✗	87.5	40.0
DP (Lécuyer et al. 2019)	28-10 Wide ResNet	✗	87.0	25.0
TRADES (Zhang et al. 2019)	ResNet-18	✓	84.9	56.6
PCL (Mustafa et al. 2019)	ResNet-110	✓	91.9	46.7
PNI (He, Rakin, and Fan 2019)	ResNet-20 (4x)	✓	87.7	49.1
Adv-BNN (Liu et al. 2019)	VGG-16	✓	77.2	54.6
L2P (Jeddi et al. 2020)	ResNet-18	✓	85.3	56.3
MART (Wang et al. 2020)	ResNet-18	✓	83.0	55.5
BPFC (Addepalli et al. 2020)	ResNet-18	✗	82.4	41.7
RLFLAT (Song et al. 2020)	32-10 Wide ResNet	✓	82.7	58.7
MI (Pang, Xu, and Zhu 2020)	ResNet-50	✗	84.2	64.5
SADS (S. and Babu 2020)	28-10 Wide ResNet	✓	82.0	45.6
A <sup>2</sup> SNN	ResNet-18	✗	84.4	72.0

confidence goes up. However, our A<sup>2</sup>SNN achieves the best performance in almost all cases except  $\kappa = 0.1$ . Particularly, we can see that our method outperforms L2P with large margins when the confidence is high. Overall, it further confirms the efficacy and generality of our A<sup>2</sup>SNN.

**Black-box Attack** To further verify the robustness of our A<sup>2</sup>SNN, we conduct the experiments on a black-box attack, the One-Pixel attack (Su, Vargas, and Sakurai 2019). This attack is derivative-free and relies on evolutionary optimization, and its attack strength is controlled by the number of pixels it compromises. We follow Jeddi et al. (2020) and consider pixel numbers in  $\{1, 2, 3\}$ . From the results in Table 3, we can see that again our method demonstrates the strongest robustness in all three cases, showing 7%, 9% and 10% improvement over the best competitor Adv-BNN (Liu et al. 2019). Importantly, these results show that the robustness of our method does not rely on stochastic gradients.

## 4.3 Comparison to State of the Art

Direct comparison to a wider range of competitors is difficult due to the variety of backbones and settings used. Nevertheless, Table 4 provides comparison to recent state of the art stochastic and non-stochastic defenses. We can see that A<sup>2</sup>SNN achieves excellent performance including comparing to methods that use bigger backbones and make the stronger assumption of adversarial training.

Table 5: Ablation study for FGSM and PGD attacks on CIFAR-10, SVHN and F-MNIST. Max-Entropy regularization is defined in Eq. 2, WCA regularization is defined in Eq. 4, and their linear combination is defined in Eq. 1.

			CIFAR-10			SVHN			F-MNIST		
Model	Noise	Regularizer	Clean	FGSM	PGD	Clean	FGSM	PGD	Clean	FGSM	PGD
No Def.	-	-	84.2	15.8	0.8	92.0	20.8	13.9	90.8	51.7	13.3
$m_1$	Isotropic	Max-Entropy	83.8	22.4	15.7	90.9	72.2	70.5	90.7	56.1	13.7
$m_2$	Isotropic	WCA	84.0	23.9	18.0	91.4	72.6	71.2	90.8	58.4	22.7
$m_3$	Anisotropic	Max-Entropy	81.5	58.1	54.0	91.6	76.2	75.4	91.2	62.7	15.8
$m_4$	Anisotropic	WCA	82.8	51.6	47.9	91.6	86.5	84.1	90.5	60.2	21.5
$m_5$	Anisotropic	Both	84.4	73.3	72.0	91.5	86.8	84.4	90.8	77.5	43.9

Table 6: Control experiments for further analysis. Conditions as per Table 5. See text for details.

Experiment	Clean	FGSM	PGD
A <sup>2</sup> SNN ( $m_5$ )	84.4	73.3	72.0
Multiple noise samples	83.6	69.2	68.6
Noise trained independently	83.8	72.1	70.3
No EoT	83.8	78.5	76.5
A <sup>2</sup> SNN: AT	78.5	35.7	31.7
A <sup>2</sup> SNN: CT+AT	80.7	36.0	29.2

#### 4.4 Further Analysis

**Ablation Study** We perform a thorough ablation study on three benchmarks, CIFAR-10, SVHN and F-MNIST, to investigate the contributions of the components we introduced in Section 3. From the results in Table 5, we can make the following observations: (i) Employing a max-entropy regularizer with isotropic noise ( $m_1$ ) already improves the model robustness under both FGSM and PGD across all three benchmarks, similarly to previously reported results (He, Rakin, and Fan 2019). (ii) Our results further show that injecting anisotropic noise benefits model robustness much more than the corresponding isotropic variant, according to the comparison between  $m_1$  and  $m_3$ . (iii) The WCA regularizer  $m_4$  shows a comparable effect to the max-entropy one  $m_3$ . (iv) Finally, we can see that all the techniques we proposed are complementary and produce the best results as  $m_5$ , which is the full A<sup>2</sup>SNN model.

All the FGSM and PGD attacks in Table 5 use attack strength  $\epsilon = 8/255$ . For completeness, we report the performance of all the variants above against FGSM and PGD with various attack strengths  $\epsilon = 2^n$ ,  $n \in \{0 \dots 7\}$  on CIFAR-10 shown in Figure 1. From these results, we can see the overall trend here is consistent with the observations in Table 5. Also, we can see that the performance of our variants degrades more gracefully than the defenseless baseline.

**Importance of EoT** To verify the efficacy of EoT, we also evaluate the test performance without it. Table 6 shows that the test performance increases without using EoT. This makes sense as critiqued in Athalye, Carlini, and Wagner (2018); one sample of gradients is not enough to construct

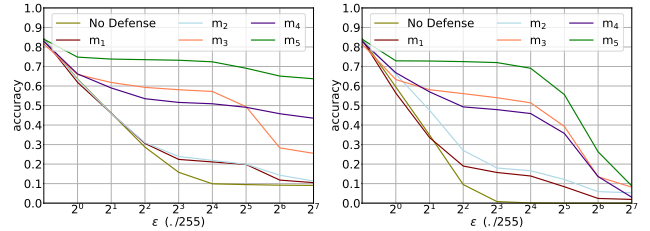


Figure 1: Evaluation of our model variants (see Table 5) for different attack strengths  $\epsilon = 2^n$ ,  $n \in \{0 \dots 7\}$ , specifically for the FGSM (left) and PGD (right) attacks on CIFAR-10. Best viewed in color.

an effective attack.

**Average multiple noise samples at test** Our model’s forward pass performs the following: (i) Extract features from the penultimate layer of the backbone, (ii) inject additive noise, and (iii) compute the logits. By default we draw a single noise sample as suggested by our theory. In this experiment, we sample from the distribution multiple times and average the final logits. The more samples we average, the more we expect the additive noise to lose its regularization effect. The experimental results in Table 6 confirm that using more ( $n = 10$ ) samples degrades performance.

**Train noise and model independently** In this experiment, we first train the model without injecting any noise. Then, keeping the model parameters frozen we train the noise independently. Table 6 shows that the accuracy scores of this experiment are comparable to the joint training (Table 5), albeit slightly lower. This confirms that the benefit of our approach is primarily due to the learning theoretic effect outlined in Section 3.2, and not largely due to any implicit feature regularization effect (Neelakantan et al. 2015).

**Adversarial training** Our proposed A<sup>2</sup>SNN only requires clean data for training. To show this, we train our best variant with PGD in two settings: purely adversarial training (AT) and mixed clean and adversarial training (CT+AT). From the results in Table 6, we can see that incorporating adversarial training harms our performance on clean data as expected (Goodfellow, Shlens, and Szegedy 2015); while providing no consistent benefit for adversarial defense.

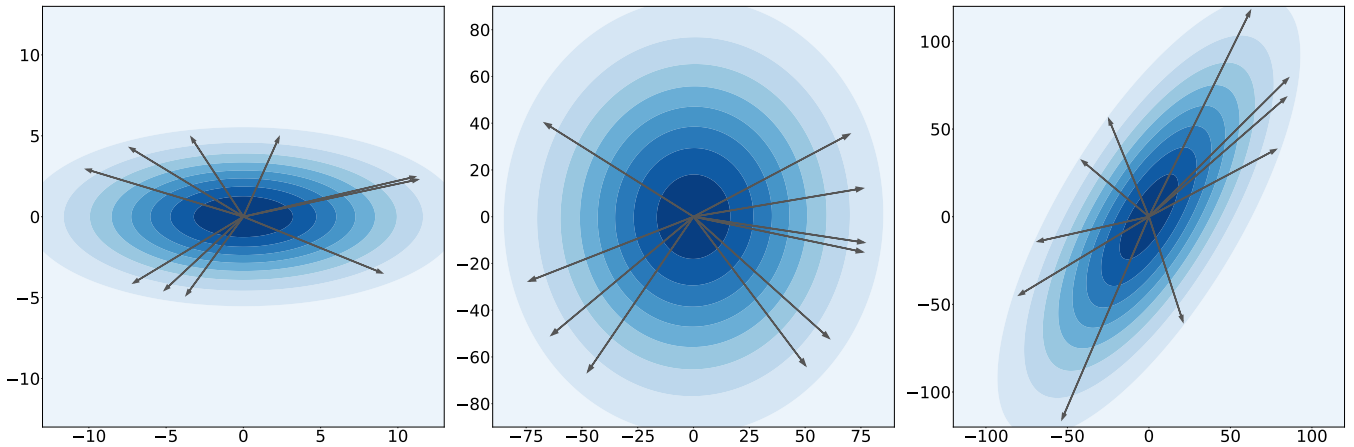


Figure 2: Visualisation of our models on F-MNIST with a 2D bottleneck. Contours and arrows indicate noise covariance  $\Sigma$  and weights  $\vec{w}_i$ . Left:  $m_2$  (isotropic with WCA). Middle:  $m_3$  (anisotropic with max-entropy). Right:  $m_5$  (anisotropic with both WCA and max-entropy). Only our full A<sup>2</sup>SNN ( $m_5$ , right) allows noise to be aligned with off-axis weights.

#### 4.5 Inspection of Gradient Obfuscation

Athalye, Carlini, and Wagner (2018) proposed a set of criteria to inspect whether a stochastic defense method relies on obfuscated gradients. Following He, Rakin, and Fan (2019), we summarize these criteria as a checklist. If any item in this checklist holds true, the stochastic defense is deemed unreliable. The following analysis verifies that our model’s strong robustness is not caused by gradient obfuscation.

**Criterion 1:** One-step attacks perform better than iterative attacks.

**Refutation:** From the results in Tables 1, 5 and 6, we can see that our A<sup>2</sup>SNN performs consistently better against FGSM than against PGD.

**Criterion 2:** Black-box attacks perform better than white-box attacks.

**Refutation:** From Tables 1 and 3 we observe that FGSM and PGD outperform the 1-pixel attack. In Figure 1 we see the effect of increasing the attack strength on both white-box attacks, and they still outperform the stronger 2- and 3-pixel attacks.

**Criterion 3:** Unbounded attacks do not reach 100% success.

**Refutation:** For fair comparison to previous work, FGSM and PGD in this paper are parameterized following He, Rakin, and Fan (2019). However, if we increase the attack strength of PGD to  $\epsilon = 255/255$  and number of iterations to  $k = 20$ , all of our examined models in the ablation study reach zero accuracy.

**Criterion 4:** Random sampling finds adversarial examples.

**Refutation:** To assess this, we hand-pick 100 CIFAR-10 test images that our model successfully classifies during standard testing (100% accuracy), but misclassifies under FGSM with  $\epsilon = 8/255$  (0% accuracy). For each of these test images, we randomly sample 10,000 perturbed images within the same  $\epsilon$ -ball, and replace the original image if any of the samples result in misclassification. We then evaluate our model on these 100 images to get a performance of 97%.

**Criterion 5:** Increasing the distortion bound doesn’t increase success.

**Refutation:** Figure 1 shows that increasing the distortion bound increases the attack’s success.

#### 4.6 Empirical Observations about WCA

Figure 2 shows the effect of our regularization methods with a bivariate Gaussian, by plotting the contours of the distribution against the weight vectors of the classification layer. These visualizations are obtained by training our  $m_2$ ,  $m_3$  and  $m_5$  models with a LeNet++ backbone on F-MNIST, with a 2-dimensional bottleneck and 2x2 covariance matrix.

We show the following: (i) First, in the left of Figure 2, we can see that the learned noise is axis-aligned since  $m_2$  injects isotropic noise. Further, we can see that the weight vectors are near-axis-aligned, as WCA pushes them to align with the learned noise. (ii) In the middle Figure, we can see that because  $m_3$  uses max-entropy regularization, the learned anisotropic noise is inflated in both dimensions. However, max-entropy regularization encourages the noise to be near-spherical despite the full covariance; consequently, it is seen that one dimension of the variance is redundant because it is not weight-aligned. (iii) In the right Figure, due to the combination of anisotropic noise and WCA, our main model A<sup>2</sup>SNN ( $m_5$ ) has weight-aligned noise, and the weights are free to be non-axis-aligned. Overall, we observe the best alignment between the learned weight vectors and the eigenvectors of the covariance matrix in A<sup>2</sup>SNN.

## 5 Conclusions

In this paper we contribute the first stochastic model for adversarial defense that features fully-trained, anisotropic Gaussian noise and does not rely on adversarial training. We provide both theoretical support for the core ideas behind it, and experimental evidence of its excelling performance. We extensively evaluate A<sup>2</sup>SNN on a variety of white-box and black-box attacks, and further show that its high performance is not a result of stochastic (obfuscated) gradients. Thus, we consider the proposed model to push the boundary of adversarial robustness.

## References

- Addepalli, S.; S., V. B.; Baburaj, A.; Sriramanan, G.; and Babu, R. V. 2020. Towards Achieving Adversarial Robustness by Enforcing Feature Consistency Across Bit Planes. In *CVPR 2020*.
- Athalye, A.; Carlini, N.; and Wagner, D. A. 2018. Obfuscated Gradients Give a False Sense of Security: Circumventing Defenses to Adversarial Examples. In *ICML 2018*.
- Biggio, B.; Fumera, G.; and Roli, F. 2013. Security evaluation of pattern classifiers under attack. *IEEE transactions on knowledge and data engineering* 26(4): 984–996.
- Carlini, N.; and Wagner, D. A. 2017. Towards Evaluating the Robustness of Neural Networks. In *SP 2017*.
- Chen, P.-Y.; Zhang, H.; Sharma, Y.; Yi, J.; and Hsieh, C.-J. 2017. Zoo: Zeroth order optimization based black-box attacks to deep neural networks without training substitute models. In *ACM 2017*.
- Cohen, J.; Rosenfeld, E.; and Kolter, Z. 2019. Certified Adversarial Robustness via Randomized Smoothing. In *International Conference on Machine Learning*, 1310–1320.
- Goodfellow, I. J.; Shlens, J.; and Szegedy, C. 2015. Explaining and Harnessing Adversarial Examples. In *ICLR 2015*.
- Gouk, H.; and Hospedales, T. M. 2020. Optimising Network Architectures for Provable Adversarial Robustness. In *SSPD 2020*.
- He, K.; Zhang, X.; Ren, S.; and Sun, J. 2016. Deep Residual Learning for Image Recognition. In *CVPR 2016*.
- He, Z.; Rakin, A. S.; and Fan, D. 2019. Parametric Noise Injection: Trainable Randomness to Improve Deep Neural Network Robustness Against Adversarial Attack. In *CVPR 2019*.
- Jeddi, A.; Shafiee, M. J.; Karg, M.; Scharfenberger, C.; and Wong, A. 2020. Learn2Perturb: An End-to-End Feature Perturbation Learning to Improve Adversarial Robustness. In *CVPR 2020*.
- Kingma, D. P.; and Welling, M. 2014. Auto-encoding variational bayes. In *ICLR 2014*.
- Krizhevsky, A.; Hinton, G.; et al. 2009. Learning multiple layers of features from tiny images. *Toronto.edu [Online]*. Available: <https://www.cs.toronto.edu/~kriz>.
- Kurakin, A.; Goodfellow, I. J.; and Bengio, S. 2017. Adversarial examples in the physical world. In *ICLR 2017*.
- LeCun, Y.; Cortes, C.; and Burges, C. 2010. MNIST handwritten digit database. *ATT Labs [Online]*. Available: <http://yann.lecun.com/exdb/mnist>.
- Lécuyer, M.; Atlidakis, V.; Geambasu, R.; Hsu, D.; and Jana, S. 2019. Certified Robustness to Adversarial Examples with Differential Privacy. In *SP 2019*.
- Lee, G.-H.; Yuan, Y.; Chang, S.; and Jaakkola, T. 2019. Tight certificates of adversarial robustness for randomly smoothed classifiers. In *Advances in Neural Information Processing Systems*, 4910–4921.
- Li, B.; Chen, C.; Wang, W.; and Carin, L. 2019. Certified adversarial robustness with additive noise. In *Advances in Neural Information Processing Systems*, 9464–9474.
- Liu, X.; Cheng, M.; Zhang, H.; and Hsieh, C. 2018. Towards Robust Neural Networks via Random Self-ensemble. In *ECCV 2018*.
- Liu, X.; Li, Y.; Wu, C.; and Hsieh, C. 2019. Adv-BNN: Improved Adversarial Defense through Robust Bayesian Neural Network. In *ICLR 2019*.
- Madry, A.; Makelov, A.; Schmidt, L.; Tsipras, D.; and Vladu, A. 2018. Towards Deep Learning Models Resistant to Adversarial Attacks. In *ICLR 2018*.
- Mustafa, A.; Khan, S. H.; Hayat, M.; Goecke, R.; Shen, J.; and Shao, L. 2019. Adversarial Defense by Restricting the Hidden Space of Deep Neural Networks. In *ICCV 2019*.
- Neelakantan, A.; Vilnis, L.; Le, Q. V.; Sutskever, I.; Kaiser, L.; Kurach, K.; and Martens, J. 2015. Adding Gradient Noise Improves Learning for Very Deep Networks. *CoRR* abs/1511.06807.
- Netzer, Y.; Wang, T.; Coates, A.; Bissacco, A.; Wu, B.; and Ng, A. Y. 2011. Reading digits in natural images with unsupervised feature learning. *Stanford.edu [Online]*. Available: <http://ufldl.stanford.edu/housenumbers>.
- Pang, T.; Xu, K.; and Zhu, J. 2020. Mixup Inference: Better Exploiting Mixup to Defend Adversarial Attacks. In *ICLR 2020*.
- Papernot, N.; McDaniel, P.; Goodfellow, I.; Jha, S.; Celik, Z. B.; and Swami, A. 2017. Practical black-box attacks against machine learning. In *ACM 2017*.
- Pinot, R.; Meunier, L.; Araujo, A.; Kashima, H.; Yger, F.; Gouy-Pailler, C.; and Atif, J. 2019. Theoretical evidence for adversarial robustness through randomization. In *Advances in Neural Information Processing Systems*, 11838–11848.
- S., V. B.; and Babu, R. V. 2020. Single-Step Adversarial Training With Dropout Scheduling. In *CVPR 2020*.
- Shafahi, A.; Najibi, M.; Ghiasi, A.; Xu, Z.; Dickerson, J. P.; Studer, C.; Davis, L. S.; Taylor, G.; and Goldstein, T. 2019. Adversarial training for free! In *NeurIPS 2019*.
- Song, C.; He, K.; Lin, J.; Wang, L.; and Hopcroft, J. E. 2020. Robust Local Features for Improving the Generalization of Adversarial Training. In *ICLR 2020*.
- Su, J.; Vargas, D. V.; and Sakurai, K. 2019. One Pixel Attack for Fooling Deep Neural Networks. *IEEE Trans. Evol. Comput.*.
- Szegedy, C.; Zaremba, W.; Sutskever, I.; Bruna, J.; Erhan, D.; Goodfellow, I. J.; and Fergus, R. 2014. Intriguing properties of neural networks. In *ICLR 2014*.
- Tsuzuku, Y.; Sato, I.; and Sugiyama, M. 2018. Lipschitz-margin training: Scalable certification of perturbation invariance for deep neural networks. In *NeurIPS 2018*.
- Wang, Y.; Zou, D.; Yi, J.; Bailey, J.; Ma, X.; and Gu, Q. 2020. Improving Adversarial Robustness Requires Revisiting Misclassified Examples. In *ICLR 2020*.

Wen, Y.; Zhang, K.; Li, Z.; and Qiao, Y. 2016. A Discriminative Feature Learning Approach for Deep Face Recognition. In *ECCV 2016*.

Xiao, H.; Rasul, K.; and Vollgraf, R. 2017. Fashion-MNIST: a Novel Image Dataset for Benchmarking Machine Learning Algorithms. *CoRR* abs/1708.07747.

Zhang, H.; Yu, Y.; Jiao, J.; Xing, E. P.; Ghaoui, L. E.; and Jordan, M. I. 2019. Theoretically Principled Trade-off between Robustness and Accuracy. In *ICML 2019*.

## A Proof of Theorem 1

*Proof.* The definition of  $h$  can be expanded to

$$h(\vec{x}) = \vec{w}^T f(\vec{x}) + \vec{w}^T \vec{z} + b, \quad \vec{z} \sim \mathcal{N}(0, \Sigma),$$

and be reinterpreted as

$$h(\vec{x}) \sim \mathcal{N}(\vec{w}^T f(\vec{x}) + b, \vec{w}^T \Sigma \vec{w}).$$

Going further, we can see that the distribution of the margin function is

$$m_h(\vec{x}, y) \sim \mathcal{N}(y(\vec{w}^T f(\vec{x}) + b), \vec{w}^T \Sigma \vec{w}),$$

for which the probability of being less than zero is given by the cumulative distribution function for the normal distribution,

$$P(m_h(\vec{x}, y) < 0) = \Phi\left(\frac{-y(\vec{w}^T f(\vec{x}) + b)}{\sqrt{\vec{w}^T \Sigma \vec{w}}}\right). \quad (5)$$

From the increasing monotonicity of  $\Phi$ , we also have that

$$\begin{aligned} & \max_{\vec{\delta}: \|\vec{\delta}\|_p \leq \epsilon} \Phi\left(\frac{-y(\vec{w}^T f(\vec{x} + \vec{\delta}) + b)}{\sqrt{\vec{w}^T \Sigma \vec{w}}}\right) \\ &= \Phi\left(\frac{\max_{\vec{\delta}: \|\vec{\delta}\|_p \leq \epsilon} -y(\vec{w}^T f(\vec{x} + \vec{\delta}) + b)}{\sqrt{\vec{w}^T \Sigma \vec{w}}}\right). \end{aligned}$$

Suppose the adversarial perturbation,  $\delta$ , causes the output of the non-stochastic version of  $h$  to change by a magnitude of  $\Delta_p^{\tilde{h}}(\vec{x}, \epsilon)$ . There are a number of ways, such as local Lipschitz constants (Tsuzuku, Sato, and Sugiyama 2018; Gouk and Hospedales 2020), that can be used to bound the quantity for simple networks. Substituting  $\Delta_p^{\tilde{h}}$  into the previous equation yields

$$\begin{aligned} & \max_{\vec{\delta}: \|\vec{\delta}\|_p \leq \epsilon} P(m_h(\vec{x} + \vec{\delta}, y) \leq 0) \\ & \leq \Phi\left(\frac{-y(\vec{w}^T f(\vec{x}) + b) + \Delta_p^{\tilde{h}}(\vec{x}, \epsilon)}{\sqrt{\vec{w}^T \Sigma \vec{w}}}\right). \end{aligned} \quad (6)$$

Combining Equations 5 and 6 with Equation 3 results in

$$\begin{aligned} G(\vec{x}, y) & \leq \Phi\left(\frac{-y(\vec{w}^T f(\vec{x}) + b) + \Delta_p^{\tilde{h}}(\vec{x}, \epsilon)}{\sqrt{\vec{w}^T \Sigma \vec{w}}}\right) \\ & \quad - \Phi\left(\frac{-y(\vec{w}^T f(\vec{x}) + b)}{\sqrt{\vec{w}^T \Sigma \vec{w}}}\right). \end{aligned}$$

Because the Lipschitz constant of  $\Phi$  is  $\frac{1}{\sqrt{2\pi}}$ , we can further bound  $G$  by

$$G(\vec{x}, y) \leq \frac{\Delta_p^{\tilde{h}}(\vec{x}, \epsilon)}{\sqrt{2\pi \vec{w}^T \Sigma \vec{w}}}. \quad (7)$$

□

Table 7: Values of  $\lambda_1$  and  $\lambda_2$  (Eq. 1) for all experiments in our ablation study (Table 5).

	CIFAR-10		SVHN		F-MNIST	
Model	$\lambda_1$	$\lambda_2$	$\lambda_1$	$\lambda_2$	$\lambda_1$	$\lambda_2$
m <sub>1</sub>	0.1	-	0.05	-	0.1	-
m <sub>2</sub>	-	1.0	-	0.5	-	0.5
m <sub>3</sub>	0.1	-	0.05	-	0.1	-
m <sub>4</sub>	-	1.0	-	0.5	-	0.5
m <sub>5</sub>	0.1	1.0	0.05	0.5	0.1	0.5

## B Hyperparameters of Experiments

For reproducibility, we provide the hyperparameter setup of our experiments. All experiments use a batch size of 128. For experiments on CIFAR-10 and SVHN we train for 200 epochs with a learning rate of  $10^{-2}$ , while for F-MNIST we train for 100 epochs with a learning rate of  $10^{-3}$ . The regularization weights  $\lambda_1$  and  $\lambda_2$  corresponding to Eq. 1 are given in Table 7. These values were obtained by performing grid search on a held-out validation set with the following grid:  $\lambda_1, \lambda_2 \in \{10^0, 10^{-1}, 5 \times 10^{-1}, 10^{-2}, 5 \times 10^{-2}\}$ .